RESEARCH PAPER

THE DYNAMICS OF THE ATMOSPHERIC POLLUTANTS DURING THE COVID-19 PANDEMIC 2020 AND THEIR RELATIONSHIP WITH METEOROLOGICAL CONDITIONS IN MOSCOW

N. Ye. Chubarova[1*], Ye. Ye. Androsova[1], Ye. A. Lezina[2]
[1]Faculty of Geography of Lomonosov Moscow State University, Moscow, Russia
[2]GPU «Mosecomonitoring « Environmental Protection State Agency, Moscow, Russia
***Corresponding author:** chubarova@geogr.msu.ru
Received: February 9th, 2021 / Accepted: May 25th, 2021 / Published: July 1st, 2021
https://doi.org/10.24057/2071-9388-2021-012

ABSTRACT. The relationship between the dynamics of the atmospheric pollutants and meteorological conditions has been analyzed during the COVID-19 pandemic in Moscow in spring, 2020. The decrease in traffic emissions during the lockdown periods from March 30th until June 8th played an important role in the decrease (up to 70%) of many gaseous species and aerosol PM_{10} concentrations and in the increase of surface ozone (up to 18%). The analysis of the pollutant concentrations during the lockdown showed much smoother diurnal cycle for most of the species due to the reduced intensity of traffic, especially during rush hours, compared with that before and after the lockdown. The specific meteorological conditions with low temperatures during the lockdown periods as well as the observed smoke air advection have made a considerable contribution to the air quality. After removing the cases with smoke air advection the decrease in concentration of many pollutants was observed, especially in NO_x and PM_{10}. The analysis of Pearson partial correlation coefficients with fixed temperature factor has revealed a statistically significant negative correlation between the Yandex self-isolation indices (*SII*), which can be used as a proxy of traffic intensity, and daily concentrations of all pollutants, except surface ozone, which has a statistically significant positive correlation with *SII* caused by specific photochemical reactions. In situations with *SII>2.5* more favorable conditions for surface ozone generation were observed due to smaller NOx and the higher O_3/NOx ratios at the same ratio of VOC/NOx. In addition, this may also happen, since during the Arctic air advection, which was often observed during the lockdown period, the growth of ozone could be observed due to the downward flux of the ozone-rich air from the higher layers of the atmosphere.

KEYWORDS: COVID-19 pandemic, urban pollution, aerosol, gas, lockdown, traffic emission, PM_{10}, ozone, nitrogen oxides, CO, SO_2, long-term measurements, Yandex self-isolation indices, meteorological factors

CITATION: N. Ye. Chubarova, Ye. Ye. Androsova, Ye. A. Lezina (2021). The Dynamics Of The Atmospheric Pollutants During The Covid-19 Pandemic 2020 And Their Relationship With Meteorological Conditions In Moscow. Geography, Environment, Sustainability, Vol.14, No 4, p. 168-182 https://doi.org/10.24057/2071-9388-2021-012

ACKNOWLEDGMENTS: The analysis of meteorological conditions, the development of the datasets, and the analysis of several gas species concentrations have been carried out with the partial support of the RGO grant (agreement 08/07-2020-Mo). The analysis of the gas-aerosol regime in 2020 was partially supported by the Ministry of Education and Science of the Russian Federation (grant number 075-15-2021-574). This research was performed according to the Development program of the Interdisciplinary Scientific and Educational School of M.V.Lomonosov Moscow State University «Future Planet and Global Environmental Change».

Conflict of interests: The authors reported no potential conflict of interest.

INTRODUCTION

The COVID-19 pandemic has affected the air quality, especially in large urban areas (Li et al. 2020; Mahato et al. 2020; Krecl et al. 2020; Sharma et al. 2020). The adoption of strict quarantine measures and the almost complete lockdown have been reflected in the reduction of anthropogenic emissions, including greenhouse gases emissions (https://www.icos-cp.eu/event/933), and resulted in the decrease of the content of harmful substances in the atmospheric air over several geographical regions (Zambrano-Monserrate et al. 2020; Mahato et al. 2020). As a result of the reduction in transport traffic and economic activities, an improvement in air quality was observed in a number of cities. It has been expressed in a statistically significant decrease in the concentration of major air pollutants (Jain et al. 2020; Li et al. 2020) such as nitrogen oxides, carbon dioxide, mass concentration of particulate matter (PM) with a diameter smaller than 10 and 2.5 micrometer (PM10 and PM2.5, respectively). At the same time, the specific features of meteorological conditions could also affect the variability of the concentration of pollutants (Şahin et al. 2020; Briz-Redón et al. 2020).

The objective of this study was to analyze the dynamics of atmospheric air quality in the Moscow metropolitan area during the COVID pandemic in spring-summer 2020 taking into account the changing meteorological conditions. It should be noted that in Moscow, the isolation measures were introduced gradually. Firstly, on March 30, 2020 a self–isolation regime was adopted. Secondly, on April 13, 2020 more strict measures were accepted. The quarantine ended on June 9, 2020. Since the variability of the concentration of small gaseous and aerosol species also depends on meteorological conditions, a detailed study of the dynamics of the main meteorological parameters during the pandemic was carried out for the evaluation of their role in air quality changes.

For the analysis we used the meteorological observations and the measurements of the gas-aerosol composition of the atmosphere, which were carried out at the territory of the Meteorological Observatory of the Moscow State University (MO MSU). The MO MSU is considered as a background urban station (Chubarova et al., 2014) due to its location in the green area of the MSU Botanical Garden at a distance of about 350-400 m from the nearest highway.

The data and method description

The analysis of meteorological conditions and the dynamics of atmospheric pollution during the COVID-19 pandemic in Moscow was made for the 01.01.2020–30.06.2020 period. We compared the conditions before the lockdown, during the two lockdown periods and after them. To characterize the meteorological regime during this natural experiment we used the 1-minute resolution data on air temperature, atmospheric pressure, relative humidity, partial pressure of water vapor from the Vaisala MAWS-301 automatic weather station and the standard meteorological measurements from the MO MSU dataset. The measurement errors for the air temperature and relative humidity from the Vaisala station in comparison with standard measurements are 0.2°C and 2%, respectively (Environmental and climatic characteristics… 2013). In addition, we used sun/sky photometer measurements from the AERONET (Aerosol Robotic Network) program at the MO MSU (Chubarova et al. 2011) for the evaluation of the absorption Angstrom exponent (*AAE*) over the 440-870 nm spectral range for attributing the smoke air advection.

Since the gas-aerosol composition of the atmosphere depends not only on the emissions of pollutants, but also on the direction of air advection and synoptic situation, we also analyzed the periods with quasi-homogeneous meteorological conditions (QHMC). These situations were determined taking into account for the direction of air advection, circulation mode and the absence of significant changes in meteorological parameters. In addition, we consider the meteorological indicator of the intensity of pollution dispersion (IPD) (Kuznetsova et al. 2014), which characterizes the mixing conditions in the boundary layer of the atmosphere. Its value varies from 1 to 3 and is based on a complex of meteorological parameters such as the type of atmospheric circulation, the type of stratification in the boundary layer, wind speed, and precipitation. A value of 1 corresponds to the meteorological conditions favorable to the accumulation of pollution in the atmosphere, and 3 – to the conditions of its active dispersion. The IPD was calculated using the 24-hour forecast of the COSMO[1]-Ru operational model with 1-hour resolution.

In order to more accurately identify the dynamics of the urban effect on air pollution, an additional analysis of the possible advection of the smoke air from the biomass burning areas in the process of agricultural activity was also carried out, since the properties of the smoke air differ significantly from those of typical Moscow air. The following scheme of the analysis has been applied: for separating air masses influenced by the smoke air advection we used the data service for fire monitoring (https://earthdata.nasa.gov/earth-observation-data/near-real-time/firms) based on MODIS/Terra[2] measurements. In addition, using the HYSPLIT[3] model we calculated the backward trajectories at an altitude of 500 m with a time step of 24-hour. The data at 500 m usually reflect air transport at higher altitudes up to 2-3 km, which is the typical upper aerosol height in the troposphere. The location of the fire spots is considered to be important within about 50 km distance from the trajectory line. This distance is similar to the Moscow area size and can be used as a first proxy for removing the fire advection cases. If the number of fires is small and/or the spots are located within a border of a 50-km area, in addition, the data on the AERONET absorption Angstrom exponent (*AAE*) are used. A value of *AAE*=1 was applied as the threshold for the low-temperature combustion processes of smoke aerosol (Kirchstetter et al. 2004; Sun et al. 2017). If the *AAE* values are smaller than 1, then this indicates that there is no absorption by organic carbon, which efficiently absorbs in the UV and blue spectral range. Hence, these conditions corresponds to a typical Moscow air. A detailed scheme for detecting cases of smoke aerosol is described in (Chubarova et al. 2020). Fig. 1 shows the examples of the assimilation of data on fire spots and backward trajectories for Moscow conditions. Note, that on April 4, 2020, a small number of fires were observed (Fig. 1b) along the trajectory line. However, according to the AERONET data during this day, the *AAE*=1.06, which is higher than the threshold, and therefore, this day was excluded from the sample. As a result, we identified 8 periods (March 17-18, March 25-29, April 4, April 7, April 9, April 13, April 23, and June 18), when the effects of smoke on the composition of atmospheric air were observed in the Moscow metropolitan area.

The 20-minute resolution data on mass concentrations of aerosol PM10 and various trace gases (NO, NO_2, SO_2, CO, O_3, volatile organic compounds VOCs or CHx) at the MO MSU site were provided by the «Mosecomonitoring « Environmental Protection State Agency of Russia. The site is equipped by the TEOM 1400a for PM10 measurements, by the internationally certified Russian instruments from the OPTEC company (www.optec.ru) including ME 9841 for NOx, ME 9810B for O_3, ME 9850B for SO_2, K-100 for CO. The detailed description of the instrumentation and the quality assurance procedure can be found at http://mosecom.mos.ru. In order to estimate the typical mass concentrations over these months we also analyzed the data for the previous five- year period (2015–2019). The choice of this period for the comparison is due to the fact that the air quality in Moscow has significantly improved during recent years (https://mosecom.mos.ru/wp-content/uploads/2020/07/report2019.pdf), and the comparisons of the air pollution during the lockdown period in 2020 with the earlier measurements could lead to a systematic bias. In case of CHx, a 3-year period (2017–2019) was used due to the absence of measurements in the earlier years. The analysis of the data revealed the necessity of the additional correction of data. So, we removed small negative values, the cases with more than 50% difference from the

[1] COSMO is the acronym of Consortium of Small scale Modelling
[2] MODIS/TERRA is a Moderate Resolution Imaging Spectroradiometer on board of Terra satellite
[3] HYSPLIT- is the acronym of the Hybrid Single-Particle Lagrangian Integrated Trajectory model

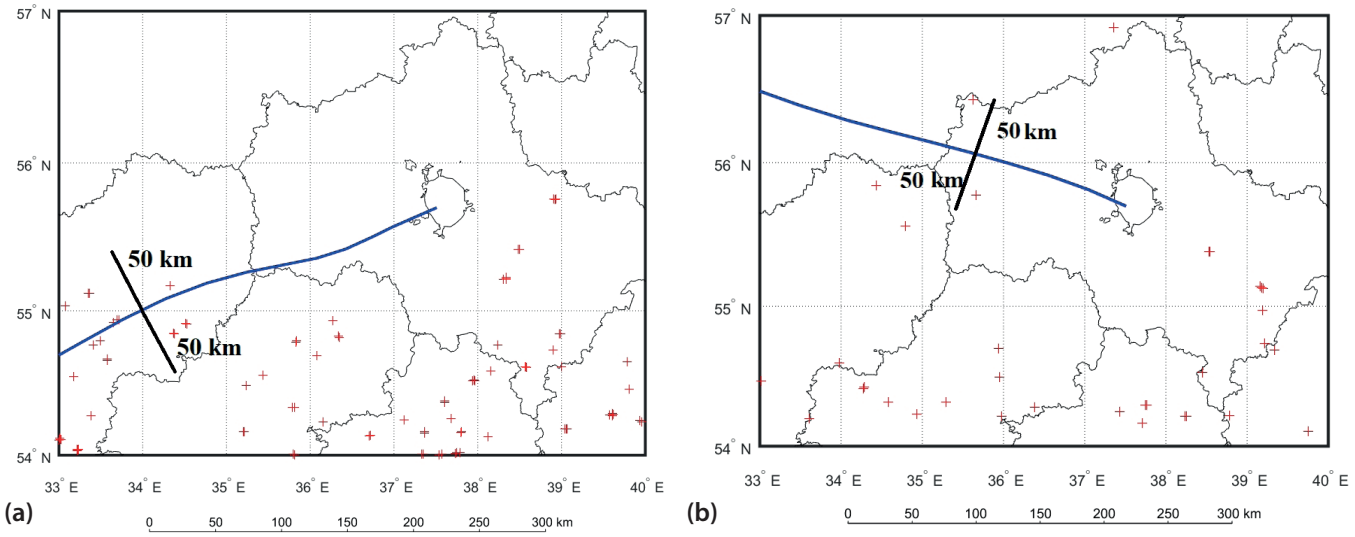

Fig. 1. The examples of data assimilation of fire locations and the direction of air particle transport for the detection of smoke advection in the Moscow region. (a) – 17/03/2020, (b) – 04/04/2020. The red marker indicates the fire centers based on satellite data from the FIRMS/MODIS dataset, the blue line – the particle 24-hour backward trajectory using the HYSPLIT model

neighboring values, zero values immediately before or after data omissions, zero values repeated two and more times in the absence of measurements simultaneously for several other parameters. In most cases, in 2020 the additional number of excluded values is small – i.e. less than 0.2% – with the exception of CO (3.1%). However, for the analyzed 5-year period, these quality criteria were not met for 17% of NO, 4% of SO_2, and 3% of CO measurements. Table 1 summarizes the total statistics on the available and removed cases. It should be mentioned that the total number of such cases, which includes the quality control tests provided at the Mosecomonitoring State Agency, are higher: from 2.9 to 22.5% depending on species for the 2015–2019 period, and from 1 to 11.9% – for 2020.

In order to characterize the main features before, within and after lockdown periods the following dates were chosen: the first lockdown period began from March, 30th – the date of the start of self-isolation regime; the second lockdown period lasted from April 13th up to June, 9th -the date of removing the self-isolation regime. These dates were determined in accordance with the Decrees of the Head of the Moscow city administration from March 29, 2020 (No. 34-UM), and the Supplement to the Decree from April 11, 2020 (No. 43-UM), and the Decree from 08.06.2020 (No. 68-UM).

In addition, the analysis of the dynamics of pollutants was carried out together with the daily values of the self-isolation index (*SII*), which was developed by the Yandex company (https://yandex.ru/company/researches/2020/podomam). The calculation of the self-isolation indices was carried out using the data from the Yandex «Transport» and «Yandex.Maps» platforms. These provide the most accurate picture of the dynamics of the transport situation in the city. Since this index is generated using the information on transport activity, it is natural to assume that it is related to the dynamics of pollutant emissions. The value has several thresholds, indicating the number of people on the street during the day. The *SII* zero corresponds to the conditions of the rush hour of a normal weekday. The *SII* from 0 to 3 qualifies the situation, when no strict lockdown conditions are observed. The *SII* from 3 to 4 qualifies the conditions, when people are rare on the streets. The *SII* in the range from 4 to 5 characterizes the conditions, when there is almost no people on the streets.

Table 1. The ratio (in %) of the additionally removed cases (N) relative to the measured case number for different pollutants. The measured case number and the number of the removed values (C / $C_{removed}$) are given in the parentheses. N_{all} – the percent of the total removed case numbers against the number of all 20-min intervals for the January-June period

Parameter	2015–2019 N% (C / Cr_{emoved}) $N_{all\%}$ (total case number =65232)	2020 N% (C / $C_{removed}$) $N_{all\%}$ (total case number =13104)
PM_{10}	0.07% (60 824 / 45) 6.8%	0.17% (12 953 / 22) 1.3%
NO	17.1% (60 927 / 10 391) 22.5%	0.01% (12 976 / 1) 1.0%
NO_2	0.07% (60 927 / 43) 6.7%	0.01% (12 972 / 1) 1.0%
SO_2	4.2% (58 322 / 2444) 14.3%	0.03% (12 955 / 4) 1.2%
CO	3.3% (62 280 / 2042) 7.7%	3.1% (11 911 / 371) 11.9%
CH_x^*	0% (37 975 / 0) 2.9%	0% (12 381 / 0) 5.5%
O_3	0.07% (55 213 / 37) 15.4%	0% (12 376 / 0) 5.6%

* for CHx the total case number is 39096 due to the shorter period of observation (2017–2019)

RESULTS

Meteorological conditions during the COVID-19 pandemic

For the Moscow region, the year 2020 was characterized by a uniquely warm winter. Table 2 shows the monthly mean meteorological characteristics for the January-June period in comparison with the long-term observations at the MO MSU from 1954 to 2013 (Chubarova et al. 2014). In winter, a stable snow cover has not been formed, since the air temperature in January and February was near zero, which was 7-8°C higher than the climatic value. In March, the average monthly air temperature also significantly exceeded the climatic value by more than 6°C. The increased air temperature affected the increase in the partial pressure of water vapor during January-March period. In April and May, on the contrary, the air temperature was slightly lower than the climatic values: by 1.4°C and 1.7°C, respectively. It happened due to the predominance of air advection from the northern regions. Low temperatures were accompanied by frequently observed low atmospheric pressure. The partial pressure of water vapor and the relative humidity were also low. In April, small amount of precipitation was recorded (22.9 mm), both relative to the climatic value, and relative to other months of 2020. In May and June, the amount of precipitation significantly, almost 3 times, exceeded the climatic value. June 2020 was characterized by warmer weather compared to the typical conditions. In general, during this month, the air temperature, and the partial pressure of water vapor were higher (by 1.5°C and 2.5 hPa, respectively) than the climatic values. The atmospheric pressure was also higher, indicating the predominance of the anticyclonic type of weather. A large amount of precipitation was associated with the active frontal systems at the beginning and at the end of June.

For a detailed analysis of weather conditions over March-June, 2020, we considered 21 periods, which were characterized by quasi-homogeneous meteorological conditions. Fig. 2 presents the variations of the meteorological parameters for these QHMC periods. During the periods of March 4-10, May 4-7, and June 4-9, there was an advection of warm and humid air masses from the southern directions. The average temperatures were about 5.8, 15.0 and 18.8°C, respectively, which is significantly higher than those in adjacent periods. The average relative humidity values were about 83, 79 and 74%. In some of these periods, the average indices of intensity of particle dispersion were significantly less than 3, reaching 2.4 during the period of May 23-28, and 2.2 – during the period of June 16-19.

During the periods of March 15-20, March 21-27, April 5-7, and May 8-22, the advection of cold and dry Arctic air masses was observed, providing a significant decrease in temperature and relative humidity in Moscow. For these periods, the average temperatures were about 3, 3, 2.2, 10.2°C, and the relative humidity comprised 56, 38, 46 and 61%, which were lower than those values in the adjacent periods. Similar conditions with the predominance of the cold air advection from the north-west direction were observed from April 12 to 29. In the periods of March 21-27, April 5-7, and May 23-28, the highest values of atmospheric pressure (i.e. >1000 hPa) were observed with the deviation from the monthly mean value by more than 15 hPa. The cyclonic circulation was the most pronounced during the period of March 11-14, when the average atmospheric pressure decreased to 975 hPa, and the deviation from the monthly mean value was -18 hPa. In the periods of May 4-7 and June 4-19, higher temperatures were observed compared with the climatic values. During the period of June, 16-19, the deviation typical conditionswas more than 5°C. The largest amount of precipitation (132.5 mm) was recorded during the period from May 29 until June 3, which comprised 37% of their total for May and June. This led to a significant excess of monthly values, especially in May, when the absolute maximum of monthly precipitation was recorded.

Figure 3 shows the average air temperature with confidence intervals at a significance level of 0.05 for the various lockdown stages during March-June 2020 compared to the 2015–2019 period. It is clearly seen, that the temperature in March (before the first stage of the lockdown) was even higher than that during the first lockdown period from March 30 until April 12, 2020. The temperature for the second lockdown period (from April 13 until June 9, 2020) was also significantly lower than the mean temperature for the 2015–2019 period. The low spring air temperature values were observed due to the prolonged influence of the cold Arctic air advection.

Table 2. Monthly mean values of meteorological parameters in January-June 2020 and their climatic characteristics for the period of 1954–2013 (adapted from Chubarova et al. 2014). For the data obtained according to long-term measurements, the values of the standard error are given in parentheses at a significance level of 0.05

	January 2020 / 1954–2013	February 2020 / 1954–2013	March 2020 / 1954–2013	April 2020 / 1954–2013	May 2020 / 1954–2013	June 2020 / 1954–2013
Air temperature (°C)	-0.2 / -8.0 (±0.96)	-0.3 / -7.5 (±0.95)	4.2 / -2.0 (±0.68)	4.8 / 6.2 (±0.57)	11.6 / 13.3 (±0.59)	18.7 / 17.2 (±0.55)
Atmospheric pressure (hPa)	988.6 / 992.4 (±1.65)	982.4 / 993.6 (±1.77)	991.8 / 993.1 (±1.46)	986.1 / 992.2 (±0.80)	988.6 / 992.4 (±0.67)	992.6 / 989.9 (±0.70)
Relative humidity (%)	85 / 83 (±0.84)	79 / 79 (±0.99)	64 / 72 (±1.23)	57 / 64 (±1.56)	66 / 61 (±1.37)	71 / 65 (±1.40)
Partial pressure of water vapor (hPa)	5.2 / 3.2 (±0.22)	4.9 / 3.1 (±0.23)	5.3 / 4.0 (±0.20)	4.9 / 6.1 (±0.25)	9.1 / 9.2 (±0.31)	15.0 / 12.5 (±0.35)
Precipitation (mm)	56 / 47 (±5.2)	35 / 40 (±5.0)	49 / 37 (±4.6)	17 / 41 (±5.1)	168 / 55 (±7.5)	193 / 76 (±8.7)

Features of atmospheric air pollution during the COVID-19 pandemic and its relationship with natural and anthropogenic factors

The main characteristics of the mass concentration of pollutants for the January-June period in 2020 and over the 2015–2019 period are summarized in Table A (in the Annex) and Fig. 4.

Before the lockdown in winter months and March, there were changes in concentrations in the range of 10-15%, with an exception of NOx and SO_2. For these species the concentrations were significantly lower (by 40-60%), and more likely due to the lower consumption of fuel for heating during the abnormally warm winter and in March. A more complex pattern was identified for ozone in January, when a significant increase (by 46%) in its concentration was observed. This could occur due to the specific features of chemical reactions at low NOx level.

In April, when quarantine measures have been already imposed and emissions significantly reduced there was a noticeable decrease up to 70%, in the concentration of almost all pollutants, except O_3, which, on the contrary, increased by 18%. The increase in O_3 during the COVID-19 lockdown periods was also reported for other geographic regions (Lee et al. 2020). In May, the picture became more complex. For some substances (NO_2, CO, SO_2, CHx, and PM10) the lower values continued to be observed, while the concentration of NO and O_3 values approached to the typical ones (to the 5-year averages). In June the concentrations of most pollutants deviated from the 5-year average in the range of 10-20%. The lowest concentrations were observed for NO_2 and SO_2 (-30 and -63%, respectively), although their concentration increased relative to the previous periods. The reason of the low values for these two species in June could be the reduction of number of cars and, possibly, an incomplete

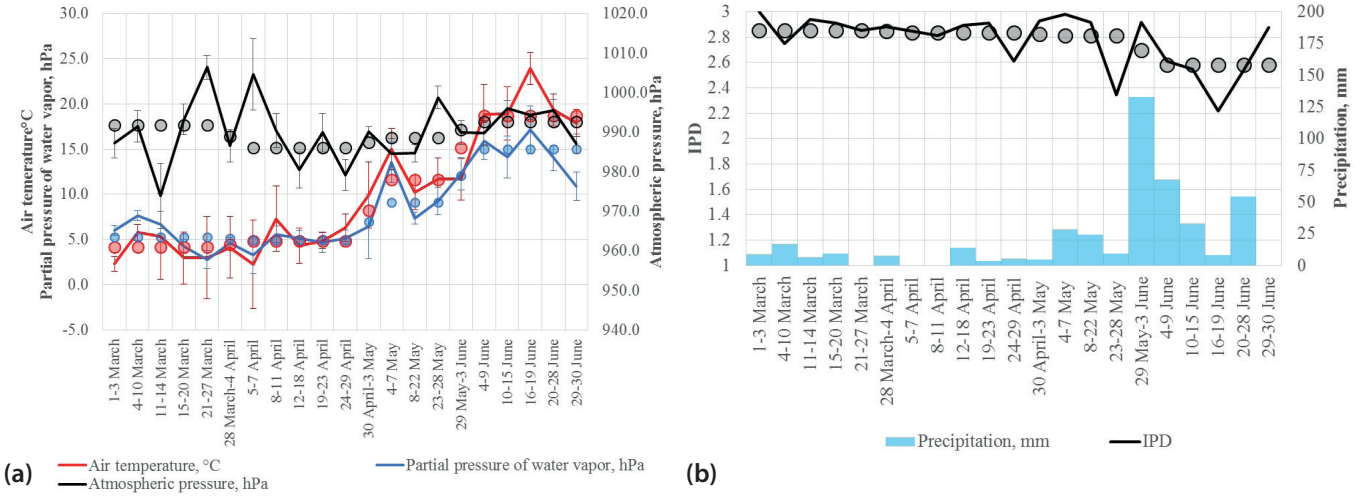

Fig. 2. Meteorological parameters (a – atmospheric pressure, air temperature, and partial pressure of water vapor; b – amount of atmospheric precipitation, and intensity of particle dispersion, (IPD) for the selected periods with quasi-homogeneous meteorological conditions, QHMC. The markers indicate the monthly mean values of the corresponding parameters

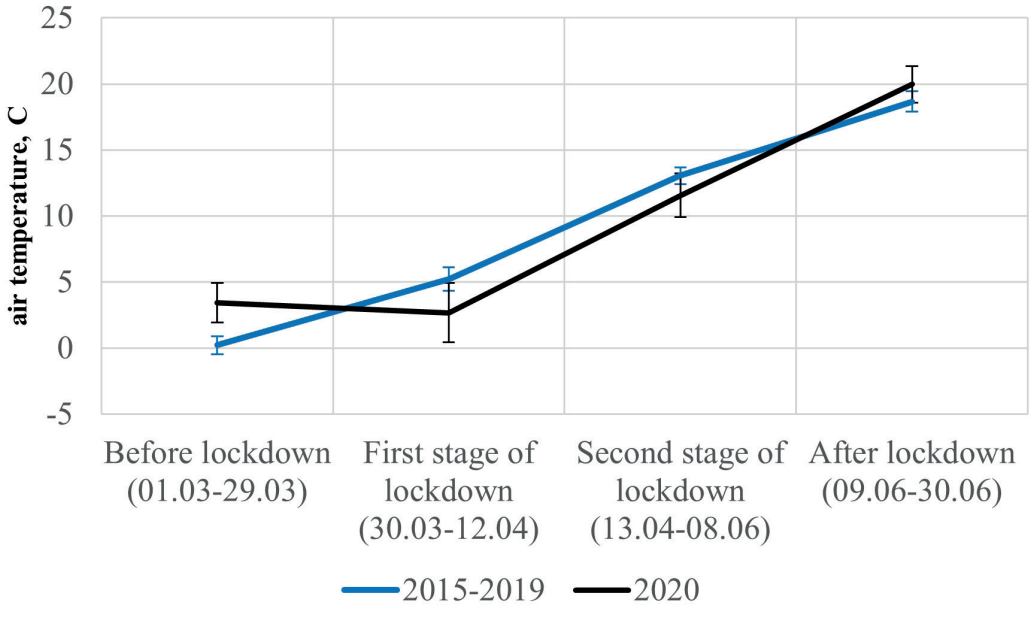

Fig. 3. The changes in the air temperature averaged over the different stages of the quarantine regime (lockdowns) in 2020 and during the 2015–2019 period in Moscow according to the measurements at the MO MSU. Confidence intervals are shown at 0.05 significance level

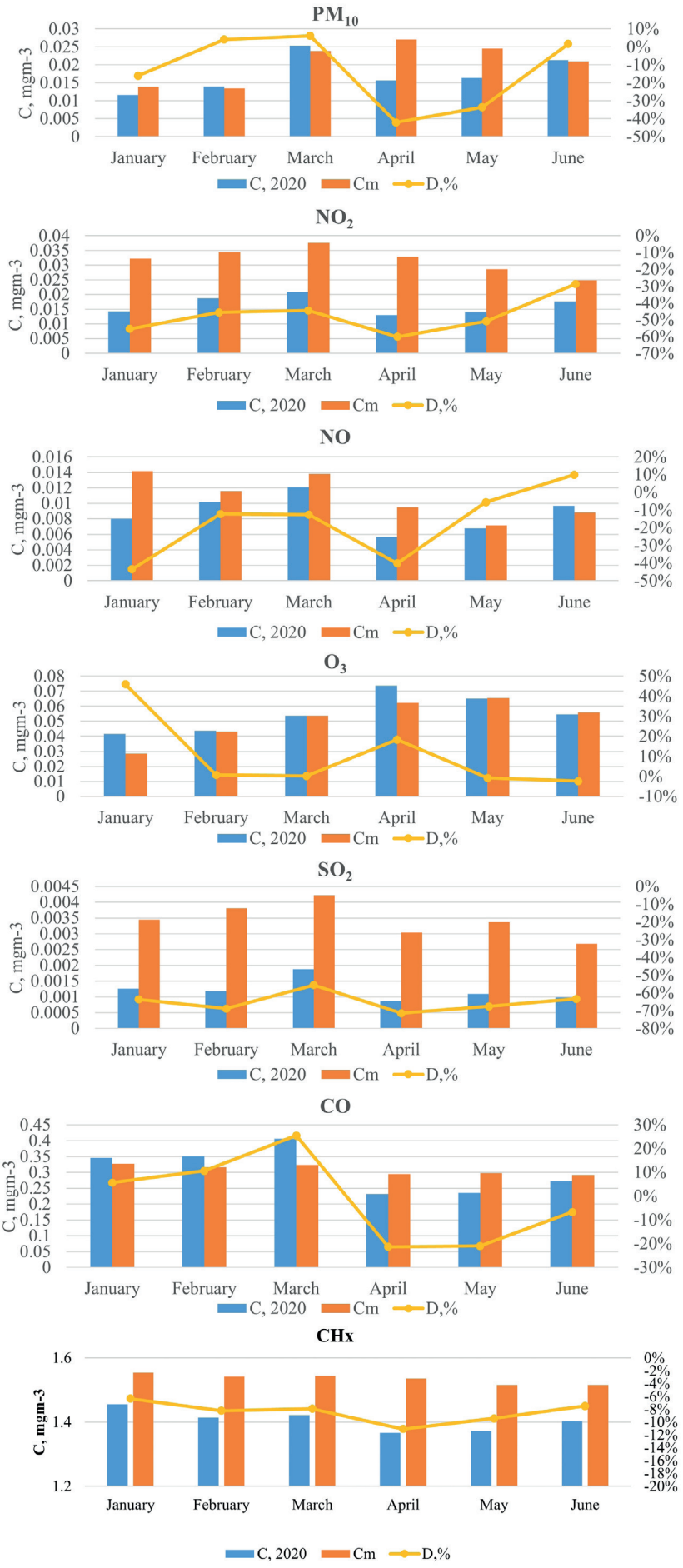

Fig. 4. Monthly mean values of the mass concentration (C, mgm^{-3}) of different pollutants – PM_{10}, NO_2, NO, O_3, SO_2, CO, CHx – observed in 2020, and in the 2015–2019 period (Cm, mgm^{-3}) and their relative differences D (in %). D=100%*(C-Cm)/Cm). Moscow

restoration of the transport activities of trucks (leading to lower emissions). Note, that the concentrations of SO_2 are extremely low in Moscow, and they are near the limit level of their detection (see Table A). The change between the relative differences of the normalized concentration between April and March (ΔD,%=D(April),%-D(March),%) was also negative for all substances, except ozone. This indicates a significant clearance of the urban atmosphere. However, the values of ΔD varied greatly: about -50% for CO and PM_{10}, about 20-30% for NOx and SO_2, and about -4% for CHx. For O_3, on the contrary, during March-April, the value of ΔD was +18%. In June a recovery in concentrations for some substances was observed. A noticeable, more than 10% increase in the normalized concentrations, compared with the May values, was observed for PM_{10} (ΔD=35%), NO (ΔD=16%) NO_2 (ΔD=22%), and CO (ΔD=14%). These changes in concentrations could be caused not only by the dynamics of anthropogenic emissions with a minimum in April-May, but also due to specific meteorological conditions during the period and the additional influence of the events with smoke advection.

For better evaluating the effects of meteorological factors we analyzed the situations for the QHMC periods. Figure 5 shows the dynamics of the average mass concentrations of pollutants and the IPD indices during these periods for all cases and for the cases without smoke advection in March-June 2020. Removing the days with smoke advection leads to a significant decrease in the concentrations of gaseous species (especially, NOx) and PM_{10}. For example, the extremely high concentrations of pollutants during the period of March 21-27 were observed due to a significant influence of smoke air advection. The effects of additional pollutants accumulation due to the stable atmospheric conditions (low IPD indices) can be only seen during the periods of May, 23-28 and June, 16-19. During these periods the average IPD values were below 2.5 and the increased concentrations of pollutants were recorded (see Figure 5b). On the whole, during the March-June period relatively high IPD indices were observed, indicating that there were no long-term conditions favorable for the accumulation of pollutants.

The lowest values of PM_{10}, SO_2, and CO were observed during the April 12-18, April 19-23 and May 8-22 periods, when there was an advection of the air from the north and north-western directions with high values of IPD.

In order to better understand the relationship between different pollutants and IPD indices we evaluated the correlation matrix between them using the QHMC bins for all cases and for cases without smoke advection. A good agreement is seen between the PM_{10} and NOx mass concentrations for both samples (Table 3). The high consistency of the surface concentrations of PM_{10} and NOx was also confirmed by the results of observations described in (Chubarova et al. 2019; Chubarova et al. 2020). There are statistically significant Pearson correlation coefficients between the IPD indices, PM_{10} and NOx. However, removing the cases with smoke advection provided a better agreement between them. In addition, in conditions without smoke advection one can see much more pronounced negative correlation between the O3 and NOx concentrations due to photochemical reactions in the same regime with typical organic and NOx emissions.

Fig. 6 shows the daily cycle of the pollutant concentrations evaluated for the studied periods: before lockdown, during the first and the second stages of lockdown and after lockdown. The cases with smoke advection were excluded from the analysis. In addition, the conditions with the advection of the cleanest Arctic air with potentially low values of the pollutants were considered separately in Fig. 6b. Note, that 42-45% of the days with the Arctic advection were observed during the analyzed periods, except for the first lockdown period, when 82% of days with such conditions were recorded.

In general, one can see much smoother diurnal cycle for most of the species due to the reduced intensity of traffic, especially during rush hours, smaller concentrations for all species, except O_3, during the lockdown periods, and some effects of seasonal changes.

The diurnal variability of PM_{10} is significantly lower in the lockdown periods, both when analyzing all cases and the cases, which are associated with the Arctic

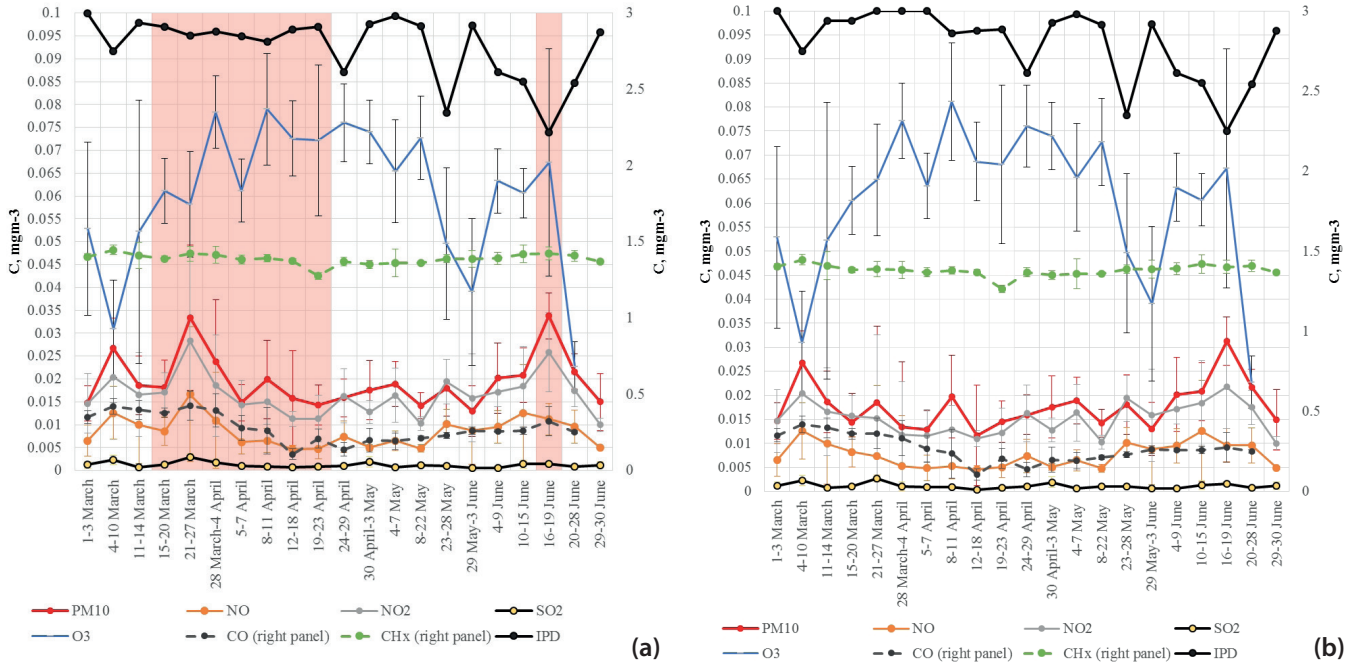

Fig. 5. Mean mass concentrations (mgm^{-3}) of pollutants – PM_{10}, NO, NO_2, SO_2, O_3, CO, CHx – and the average indices of intensity of pollution dispersion (IPD) for quasi-homogeneous meteorological periods in March-June 2020. a – all cases, b – only the cases without smoke advection. The periods, when smoke advection was observed, are marked in pink

Table 3. Correlation matrix for pollutants (PM_{10}, NO, NO_2, SO_2, CO, CHx, O_3) and the intensity of pollution dispersion (IPD) for the periods with quasi-homogeneous meteorological conditions during March-June 2020. a – all cases, b – excluding cases with smoke advection.

(a)

All cases	PM_{10}	NO	NO_2	SO_2	CO	CH_x	O_3	IPD
PM_{10}	1	**0.79**	**0.89**	**0.66**	0.56	0.62	-0.12	-0.47
NO		1	**0.91**	0.60	**0.68**	**0.74**	-0.41	-0.42
NO_2			1	0.58	0.60	**0.67**	-0.28	-0.52
SO_2				1	0.57	0.41	-0.05	-0.02
CO					1	0.64	-0.35	0.08
CHx						1	-0.46	-0.34
O_3							1	0.18
IPD								1
n	21							
p	0.95	**0.999**						

(b)

No fires	PM_{10}	NO	NO_2	SO_2	CO	CH_x	O_3	IPD
PM_{10}	1	**0.65**	**0.79**	0.46	0.29	0.50	-0.27	**-0.66**
NO		1	**0.89**	0.24	0.46	**0.70**	**-0.64**	-0.60
NO_2			1	0.27	0.34	0.59	-0.53	**-0.71**
SO_2				1	0.46	0.32	-0.06	-0.05
CO					1	0.55	-0.41	0.19
CHx						1	-0.52	-0.30
O_3							1	0.23
IPD								1
n	21							
p	0.95	**0.999**						

advection. The increased aerosol concentration outside the lockdown periods during such advection may be associated with more active urban aerosol generation due to increased anthropogenic emissions and some effects of seasonal changes, which provides higher PM generation in warm conditions after lockdown. For NOx and CHx, which concentrations are directly related to motor transport emissions, the smoothed morning and evening peaks are associated with the decreased traffic density in the lockdown period. This tendency is most pronounced in case of the Arctic advection. Note, that during the lockdown periods in the latter conditions, the concentrations of these chemical species outside of rush hours are close to those observed in typical situations. The diurnal changes in O_3 are determined by photochemical and dynamical processes and have some seasonal features. During the lockdown period, elevated O_3 values are observed throughout the day. It is due to the specific chemical reactions in the absence of large emissions of NOx. In the diurnal cycle, the maximum is observed during the daytime at any conditions. Note, that before the lockdown the smaller diurnal O_3 maximum is associated with a lower rate of photochemical reactions at low levels of UV radiation during the cold period, which is typical for the Moscow metropolitan area conditions (Elansky et al. 2018).

The opposite dependence with higher O_3 concentrations was observed during the lockdown periods partly due to lower NOx emissions, which also provided much more smoothed diurnal O_3 cycle. For cases with the Arctic advection, the O_3 concentrations are close to those observed before the lockdown. This is probably due to the influence of a downward flux of the ozone-rich air from the upper atmosphere during the Arctic advection. Hence, the natural factors play here an important role.

The CO concentrations were lower than before and after the lockdown. However, during the first period of the lockdown they were higher than those during the second stage. This may be explained by more active chemical loss of CO due to hydroxyl, which concentration was higher in May-June at increased levels of solar radiation.

In the diurnal cycle CO and CHx had much more smoother character during the lockdown periods without peaks during rush hours, and their concentrations were lower. The concentrations of CHx during the first and second stages of the lockdown were slightly reduced (by

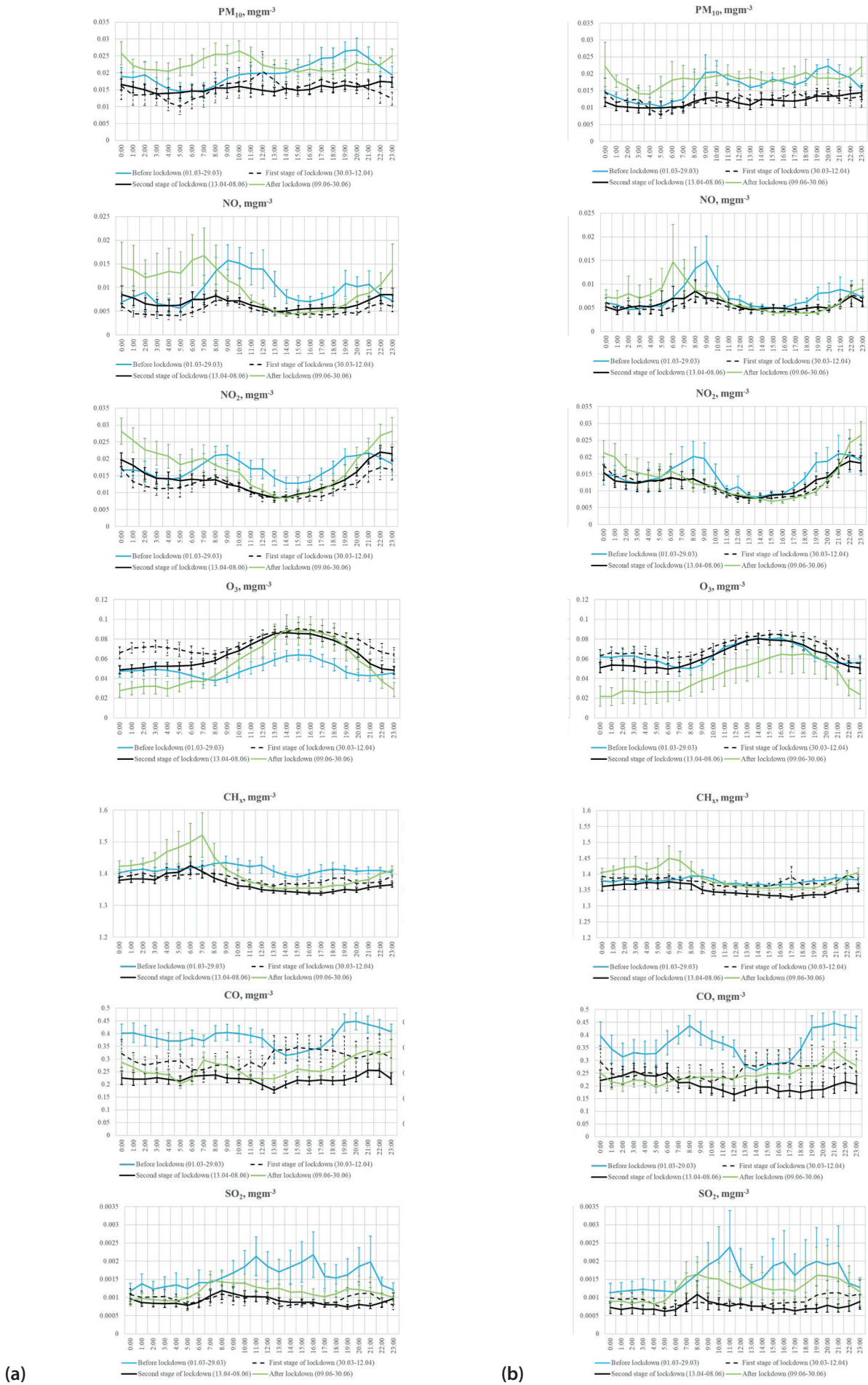

Fig. 6. Diurnal cycle of pollutants (PM_{10}, NO, NO_2, SO_2, CO, CHx, O_3) before lockdown (01.03-29.03), during the first stage of lockdown (30.03-12.04), the second stage (13.04-08.06), and after lockdown (09-30.06). a – all cases, b – only the cases with Arctic advection. The days with smoke situations were removed from the dataset

10%) to some extent due to the colder weather during these periods (see Fig. 3) and reflected smaller emission of organic matter due to lower vegetation activity.

In order to reveal the effects of emissions from traffic on the pollutants' concentrations we analyzed their relationship with the self-isolation index (*SII*) obtained from the Yandex. Figure 7 shows the *SII* dynamic during the March-June 2020 period. One can see that the *SII* values were above 2.5 during the first and partly the second lockdown periods from March 29 until May 11, 2020. At the same time, the increase in the *SII* on weekends and holidays before and after the lockdown can be sometimes as high as during the lockdown period.

The *SII* data reflect the dynamics of pollutants' emissions mainly from traffic, and, hence, the variations in concentrations of pollutants. Figure 8 shows the dependences of the daily mean concentration of various pollutants on *SII* over the March-June, approximated by a linear regression. For all species, statistically significant correlations were obtained at α=0.05, demonstrating that with the *SII* increase, the concentrations of all substances decreased. Exception is for O_3, which has a positive correlation. This result is in agreement with the analysis given above.

However, when considering the dependence only on, *SII* the changes in weather conditions were not taken into account. As shown above, during the lockdown in Moscow,

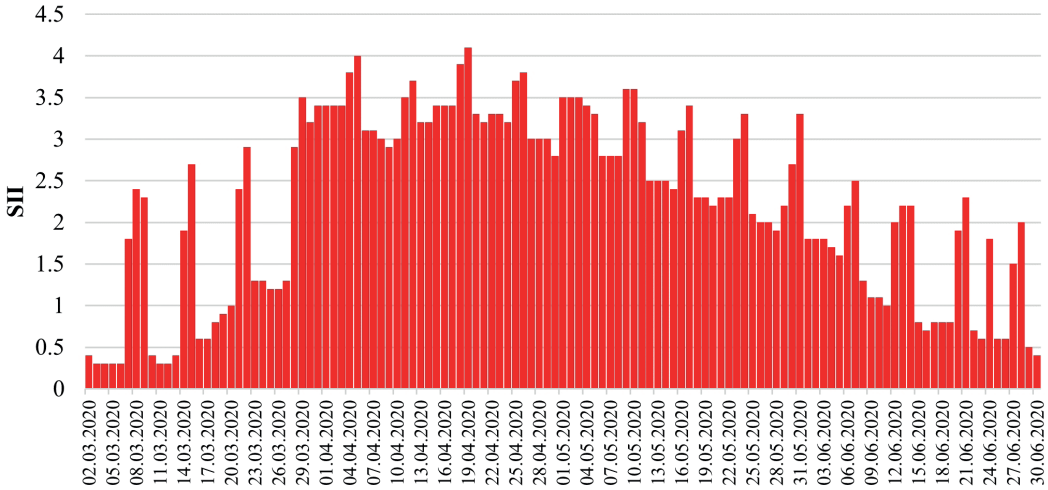

Fig. 7. The dynamics of self-isolation index (*SII*) in Moscow during March-June 2020 according to the Yandex dataset (https://yandex.ru/company/researches/2020/podomam)

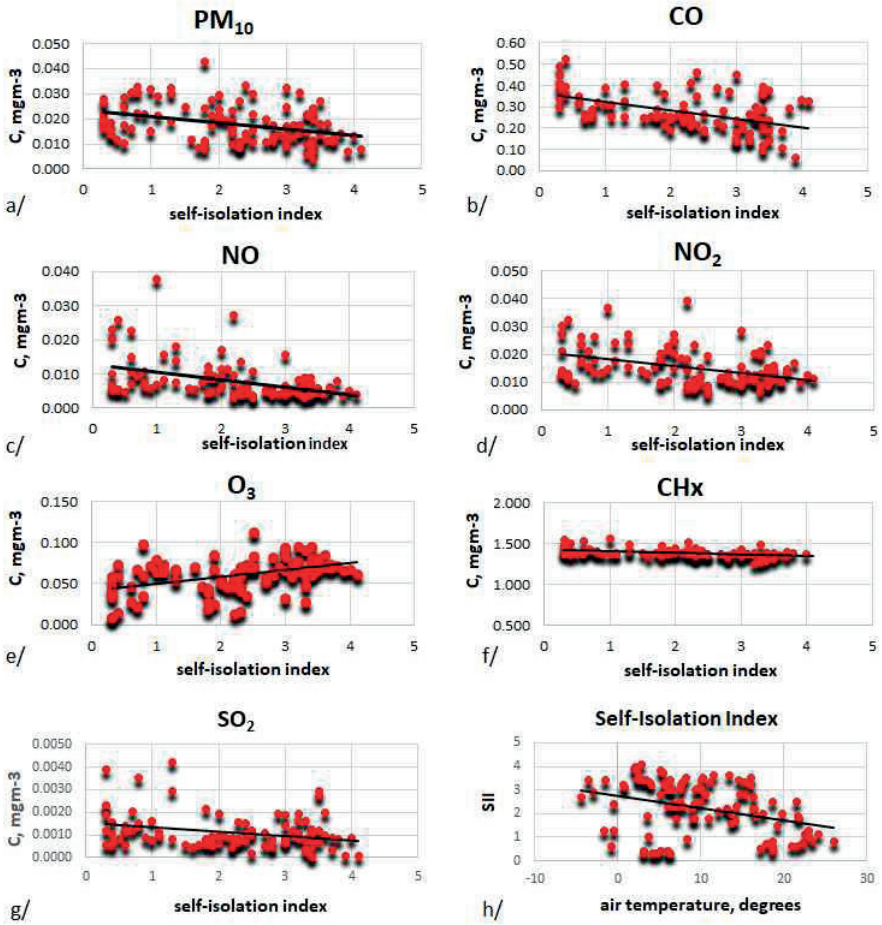

Fig. 8. The correlation between daily mean mass concentration (C, mgm^{-3}) of pollutants (PM_{10}, NO, NO_2, SO_2, CO, CHx, O_3) with self-isolation index, *SII* (a-g), and the correlation of *SII* with air temperature (h). No cases with smoke advection. March-June, 2020. Moscow

weather was characterized by cold Arctic air advection. This had an additional effect on air clearance and provided virtual *SII* dependence on the air temperature (see Fig. 8h). In order to remove the influence of the temperature changes (taken as a first proxy of different air mass advection) in variations of the pollutants' concentrations, the partial correlation coefficients were estimated. This allowed to identify the relationship between the two values at a fixed value of the third parameter (i.e. the air temperature). A comparison of the Pearson correlation coefficients between *SII* and the concentrations of pollutants with their partial correlation coefficients, when taking into account for temperature factor, is shown in Figure 9. One can see that all partial correlation coefficients remained statistically significant at α=0.05 for all species. However, in some cases, the partial correlation for coefficients were getting slightly smaller (for example, PM_{10} and NO_2) after accounting the air temperature changes.

This means that at higher temperatures, the concentrations of these pollutants are getting higher. And in some cases, on the contrary, the partial correlation coefficients increased (for example, for SO_2, CO). For SO_2, we may explain this due to large emissions of SO_2 during the heating season at relatively low temperatures. For CO, these effects were observed due to more active chemical loss in photochemical reactions during the warm period with higher temperatures at high levels of the solar radiation. As for CHx and O_3, there were no any significant changes in the sign and level of correlation coefficients. For O_3 this means that the most important factor in its dynamic is the photochemistry, and not the downward O_3 flux, which can be important only in specific conditions of the Arctic advection. Thus, we confirmed the presence of statistically significant relationships between the emissions of pollutants due to traffic, the indicator of which was the value, and the concentrations of the pollutants in the atmosphere.

A special attention was paid to the changes in concentration of surface O_3, since this is the gas of the first class of danger. Therefore, we analyzed its generation for different periods before, during, and after lockdown, as well as its changes due to *SII* variation. Fig. 10 shows the dependence of the O_3 mass concentration on NOx for different lockdown periods and *SII* ranges. In general, for all conditions we obtained non-linear relationship between O3 and NOx similar to that obtained by Zillman (1999) and Berezina et al. (2020).

The *SII* ranges qualified well the NOx limits during lockdown periods. The highest daily mean O_3 values were observed (see Fig. 10) at relatively high *SII* (>2.5), associated with a decrease in emissions of NOx. However, the O_3 generation also depends on the ratio of NOx and CHx. Figure 11 shows the ratio of O_3 concentrations to NOx as a function of ratio of CHx to NOx, which demonstrates the efficiency of O_3 formation per unit concentration of NOx at different ratios of CHx to NOx. These ratios are also given for different ranges of the *SII* values.

One can see that for all *SII* ranges, O_3 increased more efficiently with an increase in the proportion of organic compounds at the same content of NOx, which is consistent with data analysis shown by Berezina et al. (2020). At the same time, in conditions with relatively high *SII* (i.e. >2.5) the most effective O_3 generation is observed at the same CHx/NOx ratios (see Fig. 11). This may happen, since *SII*

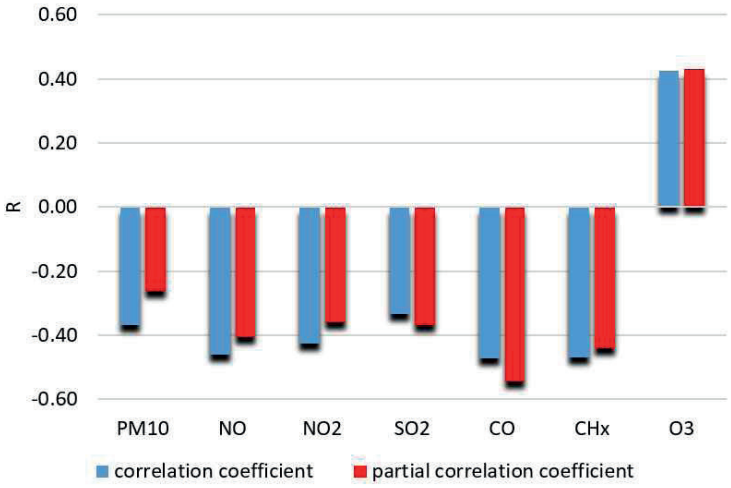

Fig. 9. The Pearson correlation coefficients between the daily mean concentration of pollutants and self-isolation index, *SII* and the partial Pearson correlation coefficients with accounting for the air temperature changes. No cases with smoke advection. All coefficients are statistically significant at α= 0.05

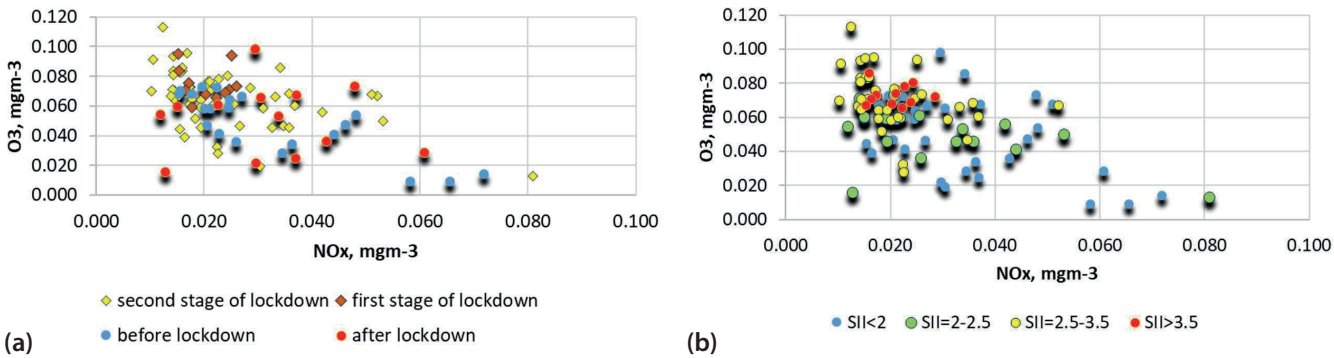

Fig. 10. The O_3 dependence on NOx concentration for different lockdown periods (a) and for different ranges of self-isolation index, *SII* (b) for the Moscow metropolitan area. Cases with smoke advection are not included

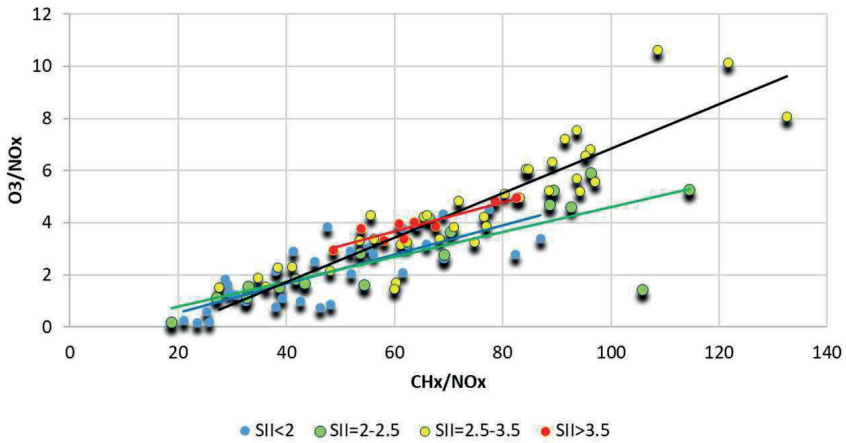

Fig. 11. The surface O_3 production per 1 mgm^{-3} of NOx at different CHx/NOx ratios for various *SII* ranges. No cases with fire advection. Moscow

values were usually higher 2.5 in April-May, 2020, when the Arctic air advection was often observed. This provided additional increase in ozone, associated with the advection of ozone-rich air from higher layers of the atmosphere.

DISCUSSION

Meteorological conditions during the analyzed period were characterized by exceptionally high monthly mean air temperatures in cold months (i.e. 6-8^{0}C above the climatic values in January-March, 2020) and the lower temperatures observed in April-May (by 1.5-2^{0}C), which affected the dynamics of the pollutants during the spring lockdown of 2020. Before the first stage of the lockdown the air temperature over the period from March, 1st until March, 30, 2020 was even higher than that during the first lockdown period (from March 30 until April 12, 2020). The temperature for the second lockdown period (from April 13 until June 9, 2020) was also significantly lower than the average temperature for the 2015–2019 period. These specific low spring air temperature conditions were observed due to the prolonged influence of the cold Arctic air advection.

In April, 2020 the average monthly mean concentrations of NO_2, NO, PM_{10}, SO_2 were 40-70% lower than those observed during the 2015–2019 period, while CO and CHx concentrations were only 10-20% lower. On the contrary, there was an increase in the concentration of surface O_3 by 18%.

The additional filters on smoke air advection resulted in removing the cases with high concentrations of pollutants (mainly, $PM1_0$ and NOx), especially at the end of March, 2020. These cases provided extremely high noise to the signal from urban pollution. The analysis without cases with smoke air advection has revealed much more pronounced relationship between O_3 and NOx, as well as between the IPD indices and concentrations of some pollutants.

The analysis of the pollutants' concentrations evaluated for considered periods before the lockdown, during the first and the second stages of the lockdown and after the lockdown provided much smoother diurnal cycle for most of the chemical species due to the reduced intensity of traffic, especially during rush hours. We also revealed the lower concentrations for all species, except O_3, during the lockdown periods, and some effects of seasonal changes in their variability. During the lockdown period, the elevated O_3 values were observed, which is due to the specific chemical reactions in the absence of large emissions of NOx. However, for the cases with the Arctic air advection, the elevated O_3 concentrations were closer to those observed before the lockdown periods due to the influence of the downward flux of ozone-rich air from the upper atmosphere in these situations.

The statistically significant negative correlation was identified between the self-isolation indices, and the daily mean concentrations of all pollutants, except surface O_3, when the positive correlation was observed. A comparison of the Pearson correlation coefficients between *SII* and the concentrations of pollutants with their partial correlation coefficients, when taking into account for the air temperature factor, revealed that the partial correlation coefficients remained statistically significant at α=0.05 for all the pollutants. However, in some cases, the partial correlation coefficients were getting slightly smaller (for PM_{10} and NOx) after accounting for the air temperature changes. This means that at higher temperatures, for example, the concentrations of these species are getting higher. In some cases, on the contrary, correlation coefficients increased (for SO_2 and CO). For SO_2, it can be explained due to larger emissions of SO_2 during the heating season at relatively low air temperatures. For CO, these effects were observed due to more active chemical loss in photochemical reactions at higher levels of the solar radiation during the warm period with the higher temperatures. For O_3, no significant changes in the sign and level of correlation coefficients were detected. This means that the process of O_3 photochemistry played more important role, than the effects of the downward O_3 flux, which can be important only in specific conditions of the Arctic air advection.

Results also showed that there is a pronounced negative nonlinear dependence of O_3 on NOx concentrations for different lockdown periods and *SII* ranges. The most active formation of O_3 was observed at the highest *SII* indices. These are associated with a decrease in emissions of NOx into the atmosphere and, accordingly, resulted in reduction of their concentration. It was also shown that for all *SII* ranges with the increase in the CHx/NOx ratio, the ozone increased more efficiently at the same content of NOx. It is consistent with results shown by Berezina et al. (2020). At the same time, the most favorable conditions for O_3 generation existed in conditions with *SII* >2.5 at the same CHx/NOx ratios. Since *SII*>2.5 were observed in April and May, we explained this feature by the additional influence of the Arctic advection during this period, which created favorable conditions for downward ozone-rich air flux from the higher layers of the atmosphere.

CONCLUSIONS

The results of our study showed that the specific meteorological conditions with extremely high air temperatures in cold months and low temperatures during the lockdown periods as well as the situation with smoke

air advection have made a considerable contribution to the air quality during the COVID-19 pandemic. Nevertheless, the decrease in traffic emissions during the lockdown periods played important role for the decrease in concentration of many pollutants and the increase in O_3 concentration. However, the growth of O_3, especially during the Arctic air advection, was observed due to natural processes of the downward flux of the ozone-rich air from higher layers of the atmosphere. The analysis of the pollutant concentrations also revealed that the lockdown periods were characterized by much smoother diurnal cycles for most of the chemical species considered due to the reduced intensity of traffic, and especially during rush hours.

A statistically significant negative relationship was obtained between the self-isolation indices, *SII* and the average daily concentrations of all pollutants, except surface O_3, which was characterized by positive correlation with . The accounting for the air temperature effects using the analysis of the partial correlation coefficients confirmed the statistically significant (at α=0.05) dependences between and the concentrations of all pollutants. It was shown that for O_3 the process of photochemistry plays more important role than the effects of the downward O_3 flux, which can be important only in specific conditions of the Arctic air advection. These relationships between the pollutant concentration and *SII* can be used in future for assessing the dynamics of urban pollution in different traffic conditions.

It was found that for all ranges with the growth of the CHx/NOx ratio, the O_3 concentration increased more efficiently at the same content of NOx. The most favorable conditions for O_3 generation were created at the same CHx/NOx ratio in conditions with *SII*>2.5. Since *SII*>2.5 were usually observed in April and May, this feature can be explained by the additional influence of the Arctic air advection during this period, which created favorable conditions for the downward ozone-rich air flux from the higher layers of the atmosphere.

REFERENCES

Berezina E., Moiseenko, K., Skorokhod A., Pankratova N.V., Belikov I., Belousov V. and Elansky N.F. (2020). Impact of VOCs and NOx on Ozone Formation in Moscow. Atmosphere, 11(11), 1262, DOI: 10.3390/atmos11111262.

Briz-Redón Á. and Serrano-Aroca Á. (2020). A spatio-temporal analysis for exploring the effect of temperature on COVID-19 early evolution in Spain. Science of The Total Environment, 728, 138811, DOI: 10.1016/j.scitotenv.2020.138811.

Chubarova N.E. Nezval' E.I., Belikov I.B. et al. (2014). Climatic and environmental characteristics of Moscow megalopolis according to the data of the Moscow State University Meteorological Observatory over 60 years. Russian Meteorology and Hydrology, 39(9), 602-613, DOI: 10.3103/S1068373914090052.

Chubarova N.E., Androsova E.E., Kirsanov A.A., Vogel B., Vogel H., Popovicheva O.B. and Rivin G.S. (2019). Aerosol and Its Radiative Effects during the AeroRadcity 2018 Moscow Experiment. Geography, Environment, Sustainability, 12(4), 114-131, DOI: 10.24057/2071-9388-2019-72.

Chubarova N., Smirnov A., Holben B. (2011). Aerosol Properties in Moscow According to 10 Years of AERONET Measurements at The Meteorological Observatory of Moscow State University. Geography, Environment, Sustainability. 4(1), 19-32, DOI: 10.24057/2071-9388-2011-4-1-19-32.

Chubarova N.E., Zhdanova E.Yu., Androsova E.E. et al. (2020). Aerosol pollution of cities and its effects on weather forecast, regional climate and geochemical processes. Moscow: MAX Press (in Russian), DOI: 10.29003/m1475.978-5-317-06464-8.

Environmental and climate characteristics of the atmosphere in 2013 according to the measurements of the Meteorological Observatory of Moscow State University. (2014). Ed. by N.Ye. Chubarova, Moscow, MAKS Press (In Russian).

Elansky N. F., N. A. Ponomarev and Ya. M. Verevkin. (2018). «Air quality and pollutant emissions in the Moscow megacity in 2005–2014», Atmos. Environ. 175, 54–64 DOI: 10.1016/j.atmosenv.2017.11.057.

Jain S. and Sharma T. (2020). Social and Travel Lockdown Impact Considering Coronavirus Disease (COVID-19) on Air Quality in Megacities of India: Present Benefits, Future Challenges and Way Forward. Aerosol and Air Quality Research, 20(6), 1222-1236, DOI: 10.4209/aaqr.2020.04.0171.

Kirchstetter T.W., Novakov T. and Hobbs P.V. (2004). Evidence that the spectral dependence of light absorption by aerosols is affected by organic carbon. Journal of Geophysical Research, 109, D21208, DOI: 10.1029/2004JD004999.

Krecl P., Targino A.C., Oukawa G.Y. and Cassino Junior R.R. (2020). Drop in urban air pollution from COVID-19 pandemic: Policy implications for the megacity of São Paulo. Environmental Pollution, 265, part B, 114883, DOI: 0.1016/j.envpol.2020.114883.

Kuznetsova I.N., Shalygina I.Yu. et al. (2014). Unfavorable for air quality meteorological factors. Proceedings of Hydrometcentre of Russia, 351, 154-172. (in Russian).

Lee J.D., Drysdale W.S., Finch D.P., Wilde S.E. and Palmer P.I. (2020). UK surface NO2 levels dropped by 42 % during the COVID-19 lockdown: impact on surface O3. Atmos. Chem. Phys., 20, 15743-15759, DOI: 10.5194/acp-20-15743-2020.

Li L., Li Q., Huang L., Wang Q. et al. (2020). Air quality changes during the COVID-19 lockdown over the Yangtze River Delta Region: An insight into the impact of human activity pattern changes on air pollution variation. Science of The Total Environment, 732, 139282, DOI: 10.1016/j.scitotenv.2020.139282.

Mahato S., Pal S. and Ghosh K.G. (2020). Effect of lockdown amid COVID-19 pandemic on air quality of the megacity Delhi, India. Science of the Total Environment, 730, 139086, DOI: 10.1016/j.scitotenv.2020.139086.

Şahin M. (2020). Impact of weather on COVID-19 pandemic in Turkey. Science of The Total Environment, 728, 138810, DOI: 10.1016/j.scitotenv.2020.138810.

Sharma S., Zhang M., Gao A.J., Zhang H. and Kota S.H. (2020). Effect of restricted emissions during COVID-19 on air quality in India. Science of The Total Environment, 728, 138878, DOI: 10.1016/j.scitotenv.2020.138878.

Sillman S. (1999). The relation between ozone, NOx and hydrocarbons in urban and polluted rural environments. Atmospheric Environment, 33(12), 1821-1845.

Sun J., Guorui Z., Hitzenberger R. et al. (2017). Emission factors and light absorption properties of brown carbon from household coal combustion in China. Atmos. Chem. Phys., 17(7), 4769-4780, DOI: 10.5194/acp-17-4769-2017.

Quinio V. and Enenkel K. (2020). How have the Covid pandemic and lockdown affected air quality in cities? [online] Centre of Cities briefing, 10th December 2020. Available at: https://www.centreforcities.org/publication/covid-pandemic-lockdown-air-quality-cities/ [Accessed 22 Jan. 2021].

Zambrano-Monserrate M.A., Ruano M.A. and Sanchez-Alcalde L. (2020). Indirect effects of COVID-19 on the environment. Science of The Total Environment, 728, 138813, DOI: 10.1016/j.scitotenv.2020.138813.

Appendix

Table A. Main statistical characteristics of the mass concentration of pollutants (in mgm-3) in 2020 and for the period of 2015–2019 according to the measurements at the MO MSU. All cases, including smoke situations.

Month	Mean 2020/ 2015–2019	Minimum 2020/ 2015–2019	Maximum 2020/ 2015–2019	50th percentile 2020/ 2015–2019	Number of cases 2020/ 2015–2019
PM_{10}					
January	0.012 / 0.014	0.001 / 0.001	0.091 / 0.094	0.009 / 0.012	2232 / 8907
February	0.014 / 0.013	0.001 / 0.001	0.133 / 0.058	0.013 / 0.012	1969 / 8568
March	0.025 / 0.024	0.001 / 0.001	0.143 / 0.464	0.020 / 0.016	2219 / 10882
April	0.016 / 0.027	0.001 / 0.001	0.083 / 0.260	0.013 / 0.021	2157 / 10665
May	0.016 / 0.025	0.001 / 0.001	0.077 / 0.185	0.014 / 0.021	2220 / 11009
June	0.021 / 0.021	0.002 / 0.001	0.109 / 0.161	0.020 / 0.007	2134 / 10748
NO					
January	0.008 / 0.014	0.001 / 0.001	0.075 / 0.329	0.006 / 0.006	2232 / 9569
February	0.010 / 0.012	0.001 / 0.001	0.057 / 0.331	0.007 / 0.006	1997 / 7702
March	0.012 / 0.014	0.001 / 0.001	0.259 / 0.353	0.007 / 0.006	2207 / 8769
April	0.006 / 0.010	0.001 / 0	0.066 / 0.275	0.004 / 0.005	2149 / 8703
May	0.007 / 0.007	0.001 / 0	0.074 / 0.199	0.005 / 0.004	2230 / 7321
June	0.010 / 0.009	0.001 / 0.001	0.128 / 0.294	0.006 / 0.006	2160 / 8472
NO_2					
January	0.014 / 0.032	0.001 / 0.001	0.052 / 0.137	0.013 / 0.030	2232 / 11156
February	0.019 / 0.034	0.003 / 0.001	0.058 / 0.125	0.016 / 0.030	1997 / 9692
March	0.021 / 0.038	0.003 / 0.002	0.164 / 0.156	0.015 / 0.032	2207 / 10941
April	0.013 / 0.033	0.002 / 0.001	0.071 / 0.155	0.011 / 0.026	2148 / 10273
May	0.014 / 0.029	0.002 / 0.001	0.064 / 0.133	0.010 / 0.022	2231 / 8927
June	0.018 / 0.025	0.002 / 0.001	0.087 / 0.144	0.013 / 0.019	2156 / 9895
SO_2					
January	0.0013 / 0.0035	0.0003 / 0.0001	0.0127 / 0.0360	0.0012 / 0.0027	2228 / 8668
February	0.0012 / 0.0038	0.0001 / 0.0001	0.0038 / 0.0790	0.0011 / 0.0030	1988 / 8702
March	0.0019 / 0.0042	0 / 0.0001	0.0161 / 0.0731	0.0013 / 0.0028	2217 / 9326
April	0.0009 / 0.0030	0 / 0	0.0084 / 0.0566	0.0007 / 0.0025	2152 / 9110
May	0.0011 / 0.0034	0 / 0	0.0089 / 0.0480	0.0009 / 0.0028	2224 / 9916
June	0.0010 / 0.0027	0 / 0.0001	0.0092 / 0.0391	0.0008 / 0.0023	2142 / 10156
CO					
January	0.35 / 0.33	0.01 / 0.10	1.73 / 2.72	0.35 / 0.30	2231 / 8930
February	0.35 / 0.32	0.02 / 0.02	0.84 / 1.92	0.34 / 0.30	1996 / 8706
March	0.41 / 0.32	0.01 / 0.01	2.41 / 2.60	0.38 / 0.30	2222 / 10442
April	0.23 / 0.29	0.01 / 0.01	0.92 / 2.50	0.21 / 0.27	1899 / 10543
May	0.24 / 0.30	0.01 / 0.01	0.91 / 2.90	0.23 / 0.25	1612 / 10951
June	0.27 / 0.29	0.02 / 0.06	1.37 / 3.37	0.25 / 0.26	1580 / 10666

CH_x					
January	1.46 / 1.55	1.28 / 1.37	1.78 / 2.81	1.45 / 1.52	2228 / 6613
February	1.41 / 1.54	1.34 / 1.36	1.91 / 2.46	1.40 / 1.52	1997 / 5732
March	1.42 / 1.54	1.32 / 1.37	2.16 / 3.22	1.40 / 1.50	2148 / 6424
April	1.37 / 1.54	1.23 / 1.21	1.67 / 2.98	1.36 / 1.52	1924 / 6383
May	1.37 / 1.52	1.22 / 1.15	2.36 / 3.21	1.35 / 1.48	1951 / 6356
June	1.40 / 1.52	1.31 / 1.08	2.75 / 3.20	1.37 / 1.49	2133 / 6465
O_3					
January	0.042 / 0.029	0.002 / 0.001	0.094 / 0.084	0.043 / 0.026	2231 / 9830
February	0.044 / 0.043	0.002 / 0.001	0.089 / 0.100	0.046 / 0.045	1979 / 7677
March	0.054 / 0.054	0.002 / 0.001	0.146 / 0.126	0.057 / 0.057	2230 / 8738
April	0.074 / 0.062	0.004 / 0.001	0.140 / 0.283	0.074 / 0.062	2158 / 10106
May	0.065 / 0.065	0.002 / 0.001	0.149 / 0.169	0.066 / 0.065	2231 / 8926
June	0.055 / 0.56	0.001 / 0.001	0.193 / 0.272	0.047 / 0.052	1547 / 9899